Horizontal Ge-Substituted Polymantane-Based C$_2$ Dimer Placement Tooltip Motifs for Diamond Mechanosynthesis

Robert A. Freitas Jr.[1,*], Damian G. Allis[2,3], and Ralph C. Merkle[4]

[1] *Institute for Molecular Manufacturing, Palo Alto, CA 94301, USA*
[2] *Nanorex, Inc., Bloomfield Hills, MI 48302, USA*
[3] *Syracuse University, Center for Science and Technology, Syracuse, NY 13244, USA*
[4] *Georgia Institute of Technology, Atlanta, GA 30332, USA*

After a systematic search for representative Ge-substituted polymantane-based carbon dimer (C$_2$) placement tool motifs for positionally-controlled vacuum diamond mechanosynthesis (DMS) using semi-empirical (AM1) and classical molecular dynamics methods, 24 potentially useful tooltip structures were examined theoretically using Density Functional Theory (DFT) to assess dimer transfer energetics, identify accessible pathological structures, and evaluate all tooltip candidates using practical engineering design criteria including tool aspect ratio, vibrational stability, and protection from hydrogen poisoning. Members of this family of 24 tooltips should be stable in vacuum and should be able to hold and position a C$_2$ dimer in a manner suitable for positionally-controlled dimer placement DMS reactions at room temperature.

Keywords: Adamantane, Carbon, Diamond, Dimer Placement, DMS, Germanium, Mechanosynthesis, Nanotechnology, Positional Control, Tooltips.

RESEARCH ARTICLE

1. INTRODUCTION

The landmark experimental demonstration of positionally-controlled atomic assembly occurred in 1989 when Eigler and Schweizer[1] spelled out the IBM logo using 35 xenon atoms arranged on a nickel surface using a scanning probe microscope (SPM). The application of precisely applied mechanical forces to induce site-specific chemical transformations is called *mechanosynthesis*, first demonstrated experimentally by Oyabu et al.[2] who employed purely mechanical forces to make and break covalent bonds, first abstracting and then rebonding a single silicon atom to a silicon surface with SPM positional control at low temperature. Positional carbon deposition on diamond surfaces has been studied computationally,[3–9] most extensively by Merkle and Freitas[6] and colleagues[7–9] who proposed the use of silicon (Si), germanium (Ge), and tin (Sn) terminated derivatives of hydrocarbon cage polymantanes as dimer placement tools in an SPM-based sub-Angstrom-precision nanopositioning apparatus for the vacuum mechanosynthesis of diamond nanostructures at room temperature via radical coupling reactions. Electronic structure calculations[6–9] and stepwise *ab initio*

molecular dynamics simulations[7–9] predict that a carbon dimer (C$_2$) covalently attached to two terminal Si or Ge atoms on at least one substituted polymantane tooltip motif should allow positionally-controlled deposition of C$_2$ onto a clean diamond C(110) surface under appropriate conditions[9] because the C–Si or C–Ge sp^3 bond between dimer and tooltip can tolerate less tensile force than the C–C sp^3 bond between dimer and substrate, hence will dissociate first, leading to covalent attachment of the C$_2$ to the substrate. Ge-linked acetylenic molecules,[10] organometallic triorganoalkylgermanes (R$_3$Ge–H),[11] polycyclic organogermanes,[12] and many other organogermanium compounds[13,14] are common in the synthetic chemistry literature. There is also a well-known and extensive literature in organosilicon chemistry,[15] including Si-substituted adamantanes.[16]

2. PRELIMINARY AM1-BASED SEARCH FOR USEFUL TOOLTIP MOTIFS

We performed a systematic search for geometrically realizable monadic horizontal dimer placement tooltip structures for diamond mechanosynthesis (DMS): (a) using diamondoid (primarily adamantane or polymantane) tool bases, both to ensure convenient attachment to a larger

SPM-compatible diamond-lattice handle structure and to retain a clear synthetic pathway toward the practical fabrication of these tools. e.g., as proposed by Freitas,[17] and (b) using Ge as the dimer-holding substituent atom, as appears optimal for single-bonded dimer-holding base structures among the choices of C, Si, Ge, and Sn.[9] This nonexhaustive search yielded 53 representative Ge-based dimer tooltip motifs (Fig. 1) on various base structures as follows:

(1) Diamond C(100) surface: dimer bonded to Ge/Ge substituted at positions adjacent (C100GeA, C100GeAX2, C100GeAX4), cross-trough straight (C100GeCTS), cross-trough diagonal (C100GeCTD), along-trough straight (C100GeATS), along-trough straight with 60° rotated base and 5-, 6-, or 7-atom side rings (C100GeATSr5, C100GeATSr6, C100GeATSr7), and along-trough diagonal (C100GeATD);

(2) Diamond C(110) surface: dimer bonded to substituted Ge/Ge along side (C110GeS), diagonal (C110GeD), and across (C110GeA) trough;

(3) Diamond C(111) surface: dimer bonded to bridge-head-substituted Ge/Ge at adjacent lattice-3-bonded carbons on 3-cage triangular (C111Ge3) and 5-cage linear (C111Ge5) tool bases, and dimer bonded across two cages on a 5-cage linear base (C111Ge5Two);

(4) Adamantane (dimer inserted into cage): dimer bound to (a) two para-substituted Ge atoms forming a 6-atom ring (AdamParaGe6), and (b) two ortho-substituted Ge atoms with non-crossbonded Ge atoms forming an 8-atom ring (AdamOrthoGe8);

(5) Adamantane (dimer replaces 1 cage C atom): dimer bound between (a) two lattice-2-bonded substituted Ge atoms (AdamGe22), (b) two lattice-3-bonded substituted Ge atoms (AdamGe33), and (c) one lattice-2-bonded and one lattice-3-bonded substituted Ge atoms (AdamGe23);

(6) Diamantane: dimer bound between two lattice-2-bonded substituted Ge atoms across the gap of 1,1-biadamantane (Biad11Ge22), 1,10-biadamantane (Biad110Ge22), and [3]-diadamantane (Diad3Ge22);

(7) Triamantane: dimer bound to substituted Ge/Ge atoms in (a) a monocarbon bridge using 5-atom (MCB5Ge), 6-atom (MCB6Ge), or 7-atom (MCB7Ge) shoulder rings with a "natural" 6-atom base ring, or similar bridging with a 5-atom base ring (MCB55Ge, MCB65Ge, MCB75Ge) or with a 7-atom base ring (MCB57Ge, MCB67Ge, MCB77Ge), (b) dicarbon bridge using 5-atom (DCB5Ge), 6-atom (DCB6Ge),[6] or 7-atom (DCB7Ge) shoulder rings with a "natural" 6-atom base ring, or similar bridging with a 5-atom base ring (DCB55AGe, DCB55BGe and DCB55CGe, DCB65Ge, DCB75Ge) or with a 7-atom base ring (DCBIceane7Ge, DCB57Ge, DCB67Ge, DCB77Ge), and (c) chevron bridge on C(111) (Chev111Ge) or C(110) (Chev110Ge) lattice;

(8) Tetramantane: dimer bound to (a) iso-tetramantane with overhanging 7-atom rings (TetraIsoGe7Over), (b) iso-tetramantane with centered 7-atom rings (TetraIsoGe7Cent), (c) iso-tetramantane with 6-atom rings (TetraIsoGe6),
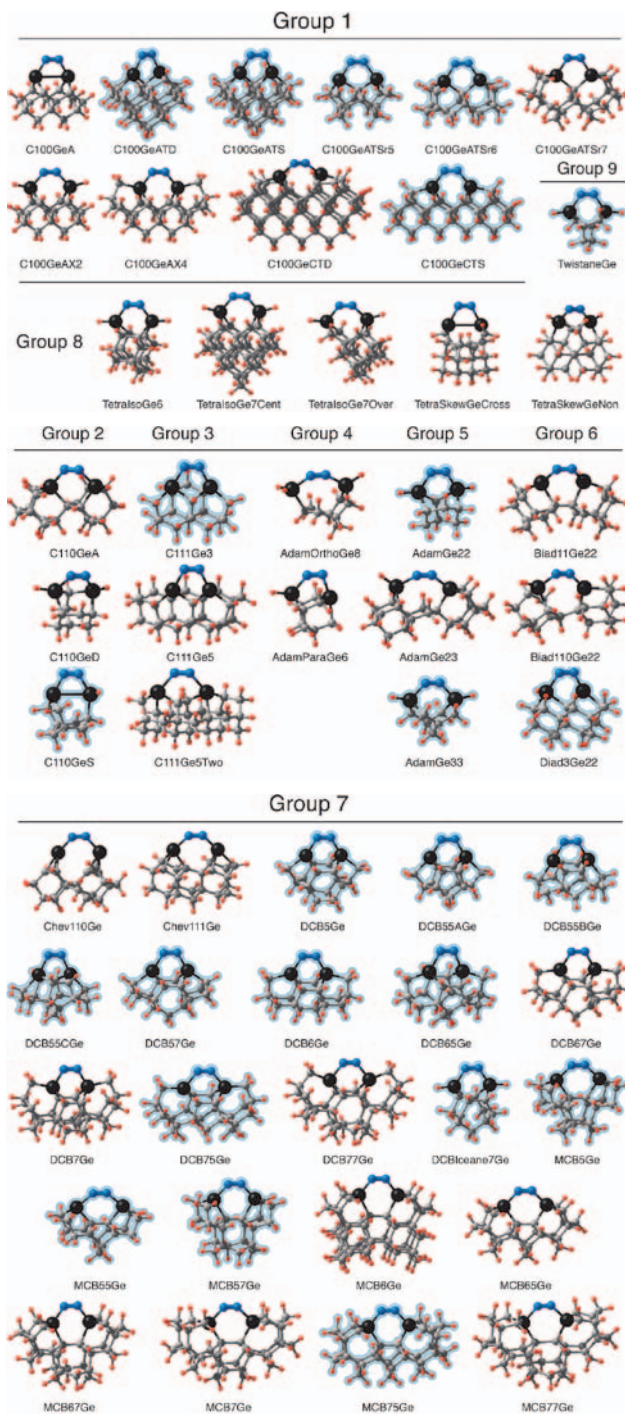

Fig. 1. 53 candidate Ge-based dimer placement tooltip motifs for positional diamond mechanosynthesis in vacuum. Potentially useful tooltip structures are highlighted.

and (d) skew-tetramantane with crossbonded (TetraSkewGeCross) and non-crossbonded (TetraSkewGeNon) substituted Ge/Ge atoms; and

(9) Twistane: dimer bonded to Ge/Ge-substituted twistane (TwistaneGe).

During use, any successful DMS tooltip molecule will be mounted on a larger rigid handle structure and

will be operated only in vacuum or other inert environment (particularly if radical sites appear during the reaction sequence) and only under continuous positional and orientational control. However, to maintain chemical stability while synthesizing the tooltip molecule in solvent phase, the C$_2$ dimer of each tooltip molecule may be passivated with a suitable capping group (e.g., I$_2$), which is subsequently removed prior to tool use in vacuum.[17]

Each of the 53 putative tooltip motifs was geometry-optimized at an AM1 (semi-empirical) level of theory[28] with tight convergence (RMS gradient 0.001 kcal/Å-mol), then pre-screened for real vibrational frequencies and possible dynamic instability using an AM1-based molecular dynamics constant-NVT simulation at 900 K in vacuum for 10 ps. This pre-screening indicated that 21 of the 53 tooltips might be structurally unstable, with 4 tooltips (C100GeAX2, MCB65Ge, TetraIsoGe6, TetraIsoGe7Cent) oscillating between carbenic (C=C:) and horizontal dimer configurations during the simulation, 8 tooltips (C100GeATSr7, C100GeAX4, DCB67Ge, DCB7Ge, DCB77Ge, MCB6Ge, MCB67Ge, MCB7Ge) stably rearranging to the carbenic form (thus are potential candidates for carbene tools in DMS), 3 tooltips (C110GeD, C111Ge5, TetraSkewGeCross) developing excessive Ge–Ge or Ge–C bond strain in the base, and 6 tooltips (AdamParaGe6, C100GeA, C111Ge5Two, Chev110Ge, Chev111Ge, MCB77Ge) indicating outright Ge–C or C–C bond-breaking in the base.

Another 8 potentially good tooltip designs were nonetheless set aside as follows: 3 tooltips (AdamGe23, AdamOrthoGe8, TetraIsoGe7Over) with one or both Ge atoms poorly constrained after dimer release (possibly remediable by adding additional base or handle structure), 4 tooltips (Biad11Ge22, Biad110Ge22, C110GeA, TetraSkewGeNon) with one or more H atoms unduly proximate to the dimer (which might not impede tool performance but could lead to lower reliability), and 1 tooltip (C100GeCTD) deemed too large (109 atoms) for practical analysis at the required levels of theory using available computational resources.

3. DFT-BASED GEOMETRY OPTIMIZATIONS FOR 24 TOOLTIP MOTIFS

The surviving 24 tooltip candidates were re-evaluated using Density Functional Theory (DFT)[25] in Gaussian 98,[18] with both singlet and triplet geometries optimized at the B3LYP/3-21G* level of theory,[26] singlet/triplet single point energy calculations performed at the B3LYP/6-311+G(2d,p) level of theory,[27] and singlet/triplet zero-point corrections added without scaling from frequency calculations at the B3LYP/3-21G* level of theory which were also used to verify the nature of the stationary point of each tooltip on its potential energy surface (PES). The accuracy of B3LYP/6-311+G(2d,p)//B3LYP/3-21G*

energies are estimated to have a mean absolute deviation of 0.14 eV,[19] which should be adequate for the purposes of this survey-type analysis. Thermal noise at room temperature is ∼0.026 eV; in conventional positionally-uncontrolled chemistry, errors on the order of 0.14 eV might well influence reaction rates and also the dominant reaction pathway taken when multiple alternative reaction pathways are present. However, in the context of the present analysis this should not be an issue because alternative reaction pathways are limited by using positional control. Encounters between the reactive tooltip and a workpiece under construction take place only at the desired position and only in the desired orientation. Alternative pathways that might otherwise occur in solution when molecules encounter each other in multiple random orientations and positions are largely eliminated by this approach. In addition, we would expect that the relative accuracy of the very similar structures compared here would be significantly better than the absolute errors generated by comparison of dissimilar structures[19]—the mean absolute deviation is computed from structures that are sometimes quite different. Scale factor correction of absolute energies would amount to ∼0.1 eV, but this uniform scaling is almost entirely offset when energies of very similar structures are compared.

Table I reports the results of the DFT tooltip absolute energy calculations for 24 tooltip motifs. For symmetrical tooltips of this type which involve only C–C and C–Ge single bonds in the tooltip base, the PES has three primary kinetically-accessible stationary points of interest as reported in prior work[6] and an additional stationary triplet structure (ethynyl) which is reported here for the first time (Fig. 2):

(A) the loaded dimer placement tooltip with the attached dimer in a horizontal position and each dimer C atom bonded to a single Ge atom,

(B) an undesired "carbenic" rearrangement with the attached dimer in a vertical position and the proximate dimer C atom bonded to both Ge atoms,

(C) the discharged tooltip after placement of the dimer on the workpiece and subsequent tool withdrawal from the surface with the dimer off the tooltip, and
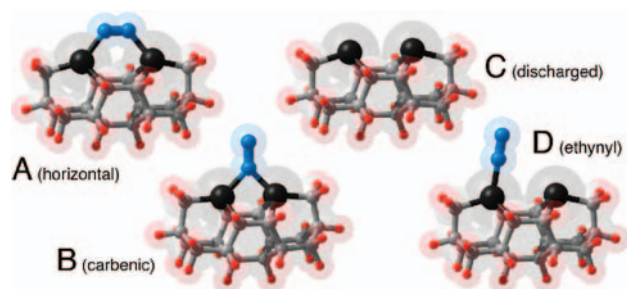

Fig. 2. (A) Horizontal, (B) carbenic, (C) discharged, and (D) ethynyl tooltip configurations for the exemplar DCB6Ge tooltip motif, showing C$_2$ dimer (blue), dimerholding Ge atoms (black), framework carbon atoms (grey), and terminating H atoms (red).

Table I. Results of DFT-based singlet and triplet total energy calculations at the B3LYP/6-311 + G(2d,p)//B3LYP/3-21G* level of theory for Ge-based dimer placement tooltip molecules. DCB6C is included as a proxy for C_2 transferred to a lonsdaleite C(111) diamond surface.

| | B3LYP/6-311 + G(2d,p)//B3LYP/3-21G* energies with zero-point correction at B3LYP/3-21G* | | | | | | |
| | Horizontal dimer | | Carbenic dimer | | Ethynyl dimer | Dimer Discharged (Off) | |
Tooltip	Singlet (eV)	Triplet (eV)	Singlet (eV)	Triplet (eV)	Triplet (eV)	Singlet (eV)	Triplet (eV)
AdamGe22	−122560.92	−122558.49	−122560.46[†]	−122557.80	−122557.68	−120488.60	−120487.26
AdamGe33	−122594.37	−122591.53	−122593.88[†]	−122591.18	—[k]	−120522.42	−120520.11
C100GeATD	−145663.59	−145661.44	−145661.93[†,d]	−145660.15[†,d]	−145662.03	−143591.21	−143591.74
C100GeATS	−145664.35	−145662.25	−145663.17[†]	−145661.13[†]	−145662.20	−143591.94	−143591.42
C100GeATSr5	−128877.66	−128876.03	−128875.73[†,d,i]	−128874.14[†,d]	−128876.45	−126805.36	−126806.10
C100GeATSr6	−133156.71	−133154.39	−133155.74[†]	−133153.30	−133153.54	−131083.39	−131083.14
C100GeCTS	−145730.51	−145727.78	−145729.75[†]	−145727.24	−145726.86	−143657.58	−143656.86
C110GeS	−123630.58	−123628.13	−123630.02[†]	−123627.37	−123627.49	−121558.04	−121557.03
C111Ge3	−132055.29	−132053.01	−132054.00[†]	−132051.76	−132052.83	−129981.87	−129982.42
DCB55AGe	−129915.29	−129913.74[e]	−129913.70[†]	−129911.41[†,f,i]	−129912.73	−127842.35	−127842.46
DCB55BGe	−132053.04[†,a]	−132051.49[e]	−132052.97	−132049.80[†,g]	−132051.25	−129980.89[†,a]	−129981.12
DCB55CGe	−133090.09	−133088.58[e]	−133088.35[†]	−133086.12[†,g]	−133088.16	−131017.76	−131017.94
DCB5Ge	−132053.44	−132050.68	−132052.10[†]	−132048.97	−132051.98[e,j]	−129980.35	−129980.05
DCB57Ge	−133091.41	−133088.94[†]	−133090.19[†]	−133087.68	−133089.06[e,j]	−131018.29	−131017.95
DCB65Ge	−135230.03	−135227.23	−135228.88[†]	−135226.20	−135226.76	−133156.64	−133156.24
DCB6Ge	−134161.98	−134159.18	−134161.24[†]	−134158.37	−134158.40	−132088.85	−132087.75
DCB75Ge	−140542.92	−140540.12	−140542.17[†,h]	−140539.44	−140539.95	−138469.67	−138468.91
DCBIceane7Ge	−126805.63	−126802.84	−126805.16[†]	−126802.34	−126801.97	−124733.25	−124731.45
Diad3Ge22	−131017.37	−131015.00	−131016.25[†]	−131010.41	−131014.57	−128943.89	−128943.68
MCB5Ge	−136299.77	−136296.75	−136298.33[†]	−136295.64	−136296.10	−134225.42	−134225.59
MCB55Ge	−133121.95	−133119.10	−133119.72[†,h]	−133117.27	−133119.58	−131048.59	−131049.17
MCB57Ge	−138438.42	−138435.47	−138437.61[†]	−138434.84	—[k]	−136365.23	−136363.85[†,b]
MCB75Ge	−147895.89	−147893.11	−147895.84[†]	−147893.04	—[k]	−145824.24	−145821.60[†,c]
TwistaneGe	−121524.39	−121521.64	−121523.78[†]	−121521.01	−121521.08	−119451.78	−119450.64
DCB6C	−23197.52	−23196.06	−23197.15	−23195.05	−23194.70	−21123.60	−21123.98
C_2 dimer	−2073.91						

[†]Transition structure. For carbene structures, motion is typically a pendulum swing in direction of horizontal dimer orientation. Uniquely for the C100GeATS carbene triplet, the fulcrum of the pendulum motion is the distal C atom of the C_2 dimer.
[a]Steric interaction of CH_2 groups at bottom of tooltip base well below the C_2 dimer, unrelated to the dimer.
[b]Ge/Ge slip above and below the Ge/Ge axis; out-of-phase oscillations in the molecular plane.
[c]Twisting motion about the Ge/Ge center; electrostatic repulsion interaction between two same-spin electrons.
[d]TS keyword used to find transition state for CarbS leading to HorS, and for CarbT leading to ethynyl rearrangement.
[e]Bond broken between Ge and C in base or shoulder.
[f]TS keyword used to find transition state for CarbT leading to tilted carbenic rearrangement.
[g]TS keyword used to find transition state for CarbT leading to HorT.
[h]TS keyword used to find transition state for CarbS leading to HorS.
[i]6-31G* basis set required for convergence of transition state.
[j]Falls to a broken horizontal triplet form; no stable ethynyl defect structure exists.
[k]Falls to the carbenic triplet form; no stable ethynyl defect structure exists.

(D) an undesired triplet "ethynyl" rearrangement with a vertical $-C{\equiv}C\cdot$ dimer bonded to just one Ge atom, leaving a monovalent radical on the other Ge atom. (The singlet "ethynyl" rearrangement is usually a very high-energy transition state on the PES and is neither stable nor accessible at or below room temperature under normal conditions of tool use—e.g., the singlet ethynyl for DCB6Ge lies +3.35 eV above the singlet carbenic form and +4.21 eV above the singlet horizontal form—so we shall not examine it further here.)

Note that the stationary points reported in Table I represent states of the tooltip in isolation and do not consider tooltip interactions with a diamond surface, an analysis that can require considerable additional computational effort.[3,7–9]

For most tooltip motifs investigated here, the undesired vertical (carbenic) rearrangement is a transition state on the PES—i.e., a frequency analysis of the stationary point shows one imaginary frequency—while both the tool-with-dimer (horizontal) and the tool-without-dimer (discharged) configurations are minima on their respective PESs, i.e., all positive real vibrational frequencies. Several exceptions should be noted. Energy minimization of the C100GeATD carbene triplet apparently leads through a nonstationary ethynyl transitional form which lies −1.88 eV below the carbene triplet transition state; however, the carbene triplet transition state also lies +1.78 eV above the preferred carbene singlet transition state and +3.43 eV above the horizontal singlet structure to which the carbene singlet proceeds apparently without barrier, hence the carbene triplet, along with the pathological ethynyl intermediate form, should remain kinetically inaccessible during normal tooltip operations at room temperature or below.

4

J. Comput. Theor. Nanosci. 4, 1–10, 2007

Geometry optimization of both the C100GeATSr5 carbene singlet transition state and the DCB55AGe carbene triplet transition state required a larger 6-31G* basis set to converge (final energy was calculated at 6-311+G(2d,p) as usual); the unusual transitional structure in the case of C100GeATSr5 (with carbenic C_2 tilted ~58° down from vertical) is noteworthy but has not been further investigated.

For most tooltip motifs the undesired triplet ethynyl rearrangement is a stationary state with no imaginary frequencies. Triplet carbene structures which have an imaginary mode of a pendulum motion back to the horizontal form are the transition structure between two forms: a horizontal triplet and the ethynyl triplet defect. In the four tooltips with highly strained Ge atoms (see discussion of singlet-triplet energy gap in Fig. 4, below), optimization of a sufficiently off-center triplet carbene optimizes to the ethynyl structure because the ethynyl transition structure removes all strain from the two Ge atoms in the triplet state. Again, several exceptions should be noted. Initial AdamGe33, MCB57Ge, and MCB75Ge triplet ethynyl structures fall directly to triplet carbene forms during energy minimization, indicating these ethynyl forms are not even stable transition states, nor are the DCB5Ge and DCB57Ge ethynyl triplets which fall to triplet horizontal forms each showing a break defect in the tooltip frame.

Finally, the DCB55BGe horizontal singlet has one imaginary frequency as a result of minor steric interactions among CH_2 groups well below the dimer in the base structure, not directly involving the C_2 dimer or Ge atoms. In the structure calculations for this small tooltip, the steric interaction leading to the imaginary frequency in DCB55BGe may be eliminated by replacing nearest-neighbor hydrogen atoms with a single bridging CH_2 group, yielding the DCB55CGe tooltip. This suggests that in an actual DMS tool assembly, covalent bonding between the DCB55BGe tooltip and the rigid covalent framework of the handle would, with the removal of the H atoms, eliminate the predicted steric interaction at the base of this tooltip.

4. DISCUSSION OF TOOLTIP UTILITY

Table II compares the mechanosynthetic reaction energetics for transferring a C_2 dimer onto an empty DCB6C molecule having two apposed monovalent bridgehead carbon radical sites on a lonsdaleite base structure—a convenient proxy for (hexagonal) diamond C(111) deposition (Fig. 3)—for all 24 new tooltip motifs reported here, plus 4 from prior studies. With three exceptions (DCB6SiGe, DCB6Si, and MCB5Ge), all tooltips show a successful exoergic dimer transfer reaction onto the model diamond surface. While it may be reasonable to presume that higher reaction exoergicity implies higher transfer reliability, note that reaction endoergicity alone does not imply tooltip unworkability. VASP stepwise-AIMD simulations[9]

of DCB6Si used to deposit C_2 dimer onto a 200-atom clean diamond C(110) surface showed that the tool is workable at 80 K, though not at 300 K, despite the small reaction endoergicity. DCB6Si remains workable because the weaker Si–C bond between tooltip and dimer cannot tolerate as high a tensile load as the stronger C–C bond between dimer and diamond workpiece, hence the former bond ruptures first during tooltip retraction, leaving the C_2 on the workpiece surface as desired. We expect MCB5Ge will also prove workable at low temperatures because its Ge–C bond between tooltip and dimer is even weaker than the similar Si–C bond in DCB6Si.

Table II shows that the ground state singlet horizontal configuration is strongly energetically preferred to the carbene triplet for all C_2-loaded tooltips, and is also strongly energetically favored to the carbene singlet in all cases except MCB75Ge and DCB55BGe (where the energy preference remains only slightly positive), hence all loaded tooltips except MCB75Ge and DCB55BGe should be very stable against carbenic rearrangement. The singlet state is also lower in energy than the triplet state for horizontal structures and for carbenic and ethynyl defect structures of all tooltips by uniformly substantial margins relative to $k_B T_{300}$ (~0.026 eV), indicating that the probability of these systems being in a triplet state at room temperature from thermal activation is negligible. The triplet ethynyl defect state is lower in energy than the triplet carbenic defect state except in the cases of AdamGe22, AdamGe33, C100GeCTS, DCBIceane7Ge, MCB57Ge, and MCB75Ge.

For discharged tooltip structures, 7 tooltips (C100Ge-ATD, C100GeATSr5, C111Ge3, DCB55AGe, DCB55BGe, MCB5Ge, and MCB55Ge) show an energy preference for the triplet over the singlet state, indicating that in these cases the two Ge radicals will not form a covalent bond across the open gap between them but will remain separated and unbonded. This wider gap should not adversely affect tooltip rechargeability because even the largest unloaded-tooltip Ge/Ge separation (4.92339 Å for MCB55Ge; Table III, column 7) is less than the combined 4.98849 Å reference Ge–C≡C–Ge bond length (linear H_3Ge–C≡C–GeH$_3$ reference structure at a B3LYP/3-21G* level of theory).

One measure of Ge–C≡C angle strain imposed on the dimer binding interaction by the rigid covalent tooltip framework is the singlet-triplet energy gap of the horizontally-bound dimer. This property of the tooltips can be easily understood using the model system H_3Ge–C≡C–GeH$_3$ (Fig. 4). As the Ge–C≡C angles are symmetrically reduced from 180 deg (linearity), the dimer π-bond in the plane of the Ge–C≡C–Ge trapezoid incorporates increasing π-anti-bonding character to account for the strained geometry of the Ge–C σ-bonds. At significant deviations from linearity, the hybridization of the dimer carbons are effectively sp^2, the condition at which the dimer π-bond in the trapezoid is broken with the π-anti-bonding orbital becoming lower in energy than the

Table II. Transfer reaction exoergicity onto a DCB6C workpiece, and singlet/triplet energy comparisons, for Ge-based (and four other) dimer placement tooltip molecules, using energies from Table I.

Tooltip	N_A	Transfer reaction exoergicity (eV)[a]	Horiz. Singlet → Carbene		Singlet → Triplet			Horiz. singlet → ethynyl triplet (eV)
			Carbene singlet (eV)	Carbene triplet (eV)	Dimer Hor. (eV)	Dimer Carb. (eV)	Dimer Off (eV)	
C100GeATSr5	35	−1.97	+1.93	+3.52	+1.63	+1.59	−0.74	+1.21
MCB75Ge	75	−1.87	+0.05	+2.86	+2.79	+2.80	+2.64	—[d]
DCB6Sn[b]	46	−1.80	+0.74	—	—	—	—	—
C100GeATD	63	−1.69	+1.66	+3.43	+2.14	+1.78	−0.53	+1.55
DCB55BGe	42	−1.61	+0.08	+3.24	+1.56	+3.17	−0.24	+1.79
AdamGe33	25	−1.58	+0.48	+3.19	+2.84	+2.71	+2.31	—[d]
DCB55CGe	43	−1.38	+1.75	+3.97	+1.51	+2.23	−0.18	+1.93
AdamGe22	23	−1.21	+0.46	+3.12	+2.43	+2.66	+1.34	+3.23
DCBIceane7Ge	33	−1.15	+0.47	+3.29	+2.78	+2.82	+1.80	+3.66
C100GeATS	63	−1.11	+1.18	+3.22	+2.10	+2.04	+0.51	+2.15
DC10c[c]	33	−1.07	+1.90	—	+1.50	—	+0.47	—
C110GeS	26	−1.00	+0.56	+3.20	+2.45	+2.65	+1.01	+3.09
TwistaneGe	22	−0.92	+0.61	+3.38	+2.75	+2.77	+1.13	+3.31
MCB55Ge	45	−0.75	+2.24	+4.68	+2.85	+2.45	−0.59	+2.38
DCB55AGe	36	−0.70	+1.59	+3.88	+1.55	+2.29	−0.11	+2.55
C111Ge3	42	−0.65	+1.29	+3.54	+2.28	+2.25	−0.55	+2.46
C100GeCTS	67	−0.60	+0.76	+3.27	+2.74	+2.51	+0.73	+3.66
DCB5Ge	42	−0.43	+1.35	+4.47	+2.76	+3.13	+0.30	—[d]
DCB57Ge	43	−0.41	+1.22	+3.73	+2.47	+2.50	+0.33	—[d]
DCB6Ge	46	−0.41	+0.85	+3.60	+2.79	+2.75	+1.10	+3.57
MCB57Ge	58	−0.33	+0.82	+3.58	+2.95	+2.76	+1.38	—[d]
DCB75Ge	62	−0.28	+0.74	+3.48	+2.79	+2.74	+0.76	+2.97
C100GeATSr6	47	−0.21	+0.97	+3.41	+2.32	+2.44	+0.25	+3.17
DCB65Ge	49	−0.14	+1.15	+3.83	+2.80	+2.68	+0.40	+3.27
Diad3Ge22	41	−0.05	+1.13	+6.96	+2.37	+5.83	+0.21	+2.80
DCB6C	46	0	+0.37	+2.46	+1.46	+2.09	−0.38	+2.82
DCB6SiGe[b]	46	+0.08	—	—	—	—	—	—
DCB6Si[b]	46	+0.58	+0.96	+3.88	+3.44	+2.92	—	—
MCB5Ge	52	+0.65	+1.44	+4.13	+3.02	+2.70	−0.17	+3.67

Singlet and triplet energies computed at B3LYP/6-311 + G(2d,p)//B3LYP/3-21G* (single point at B3LYP/6-311 + G(2d,p) with zero-point correction from frequency calculation at the B3LYP/3-21G* level of theory). N_A is the number of atoms in a C$_2$-dimer-loaded tooltip.
[a]Transfer reaction assumes tool is employed to deposit C$_2$ dimer onto an empty DCB6C tool; Reaction Exoergicity = [Min{E$_{Horiz}$(Tool/sing), E$_{Horiz}$(Tool/trip)} + E$_{Off}$(DCB6C/trip)] − [Min{E$_{Off}$(Tool/sing), E$_{Off}$(Tool/trip)} + E$_{Horiz}$(DCB6C/sing)]. [b]Data from Merkle and Freitas (2003).[6] [c]Data (or estimated) from Allis and Drexler (2005).[24] [d]No stable ethynyl defect structure exists.

highly strained electron-paired condition. Even at high angle strain, including the 115 deg to 135 deg range of these tooltips, the ground state singlet is predicted to be the lower-energy form, with the gap between singlet and triplet states indicating the degree to which the excited-state triplet is contributing to the overall description of these systems.

The singlet-triplet energy gaps for the 24 tooltips are listed in Table II. The tooltip bond angle (Table III, column 6) as a function of singlet-triplet energy gap for the horizontal configurations of all 24 tooltips is plotted in Figure 4, overlaid by curves representing the same gap for an H$_3$Ge–C≡C–GeH$_3$ reference molecule bent through a 110–140 deg range. The actual singlet-triplet energy gap in the tooltips is a function of both strain on the bound dimers and the deviation of the Ge atoms from sp^3 (tetrahedral) hybridization due to the σ-bonding framework of the tooltips themselves, with the Ge geometry accounting for much of the variation observed in the energy plot. The four tooltips deviating farthest from the idealized

H$_3$Ge–C≡C–GeH$_3$ trend are C100GeATSr5, DCB55AGe, DCB55BGe, and DCB55CGe. These four tooltips are unique from among the tooltip series for the highly non-tetrahedral geometry of their Ge atoms, whose geometries approach planarity in the horizontal singlet tooltips due to the rigidity of their attached carbon frameworks. The low observed gap in these cases are readily explained by frontier orbital analysis. In these four cases, the lowest unoccupied molecular orbital (LUMO) is a combination of both Ge atomic and dimer π-anti-bonding orbitals. In the process of relieving the large Ge hybridization strain, geometry optimization of the horizontal triplet of DCB55AGe breaks a bond between a Ge atom and a C atom in the dicarbon bridge. The considerable strain on the Ge atoms in the DCB55BGe and DCB55CGe tooltips results in the horizontal and carbene triplets of both breaking a bond between one Ge atom and its nearest CH$_2$ group in the shoulder of the tooltip structure, which deforms the remainder of each in a manner that relieves strain on the other Ge atom while retaining both Ge–C dimer bonds.
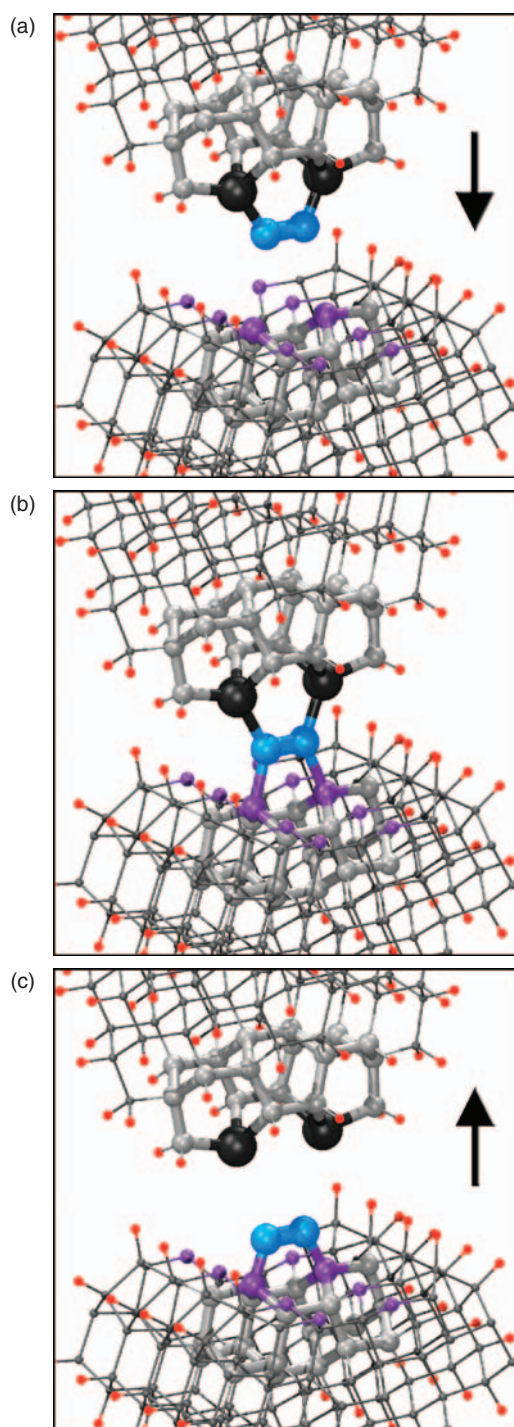
6

*J. Comput. Theor. Nanosci. 4, 1–10, **2007***

Fig. 3. In the exemplar mechanosynthetic process described here, a tooltip bearing a C$_2$ dimer payload (blue) (a) brings that payload into contact with a lonsdaleite surface across two dehydrogenated carbon monoradical sites (purple) and (b) transfers the dimer to the lonsdaleite surface; (c) the discharged tooltip is then withdrawn.

However, for all three tooltips the horizontal singlet is significantly lower in energy than the horizontal or carbene triplet (or the transition states leading to them), hence the triplet structures (which feature a broken bond) are not energetically accessible from the horizontal singlet state.

Table III collects geometric data for all 24 DFT energy-minimized Ge-based dimer placement tooltips. The C≡C bond in loaded tooltips is stretched by an average of +2.26% relative to a 1.21716 Å reference C≡C bond length (H$_3$Ge–C≡C–GeH$_3$ at B3LYP/3-21G*), ranging from a low of +1.07% for MCB75Ge to a high of +3.41% for DCB55BGe. These tensile bond strains seem modest considering the 13% C–C strains that may be found in some bonds around a Lomer dislocation in diamond[23] and the +2.7% C≡C bond stretch computed for benzyne (B3LYP/3-21G*). Similarly, the Ge–C bonds to the dimer are stretched by an equally modest average +3.02% relative to the 1.88566 Å reference Ge–C bond length (H$_3$Ge–C≡C–GeH$_3$ at B3LYP/3-21G*), ranging from a low of +0.93% for MCB75Ge to a high of +5.45% for C100GeATSr5. As a group the tooltips are extremely symmetrical, with only four candidates (C100GeATD, DCB5Ge, DCB55BGe, and TwistaneGe) having a GeC-CGe dihedral exceeding 1 deg; the Ge–C/C–Ge bond lengths to the C$_2$ dimer differ by only 0.1% in the worse case (DCB55BGe).

Another measure of tooltip utility is aspect ratio (Fig. 5), defined here as the height of the C$_2$ dimer line above the Ge/Ge line—approximated as the altitude of the Ge–C–C–Ge trapezoid, assumed planar—expressed as a fraction of the Ge/Ge separation distance (Table III, column 9). Tooltips with higher aspect ratio are more steeply "pointed," hence are better able to reach into confined spaces or to perform reliable operations on flat workpiece surfaces having numerous competing bonding sites. The average aspect ratio for all 24 tooltips is 0.522, ranging from a low of 0.343 for MCB55Ge to a high of 0.608 for C100GeATS. Reference benchmarks for aspect ratio include the C≡C position in the benzyne (C$_6$H$_4$) molecule with a similarly-calculated aspect ratio of 0.379 and a ratio of 0.464 for the trough-to-ridge altitude of a C–C ridge group on a diamond C(110) surface as estimated from a suitably rotated adamantane molecule, both using B3LYP/3-21G* geometries.

Tooltip dynamics were not extensively studied but six of the tooltips have very low vibrational frequencies of any kind, e.g., <100 cm^{-1} for the lowest ($\nu = 1$) normal mode (Table III, column 10). Such low-energy flexure might imply a larger thermal population of that mode, possibly leading to decreased predictability of dimer position during mechanosynthetic operations, hence tooltips possessing higher vibrational frequencies would be preferred. The average lowest-mode vibrational frequency for all 24 tooltips is 128.72 cm^{-1}, ranging from a low of 39.75 cm^{-1} for MCB75Ge to a high of 187.47 cm^{-1} for C100GeATD. However, this may be a weak selection criterion because many of the lowest frequency vibrations in the tooltip base may disappear when the tooltip is mounted on a larger handle structure. The lowest frequencies directly corresponding to dimer wagging or rocking motions for most of these tooltips cluster between 160–210 cm^{-1}, with

*J. Comput. Theor. Nanosci. 4, 1–10, **2007***

7

Table III. Geometric data for Ge-based dimer placement tooltip molecules after DFT energy minimization at the B3LYP/3-21G* level of theory (S = singlet, T = triplet). Loaded values are for horizontal singlet structures. Unloaded values are for discharged singlet or triplet as indicated (lowest-energy variant used). Tool aspect ratio and lowest vibrational frequency are for the horizontal singlet configuration.

Tooltip	Ge/Ge Dist. in loaded tool (Å)	C≡C Dist. in loaded tool (Å)	Ge–C≡ Dist. in loaded tool (Å)	Ge–C≡C–Ge Dihedral, loaded tool (deg)	Ge-C≡C Bond angle, loaded tool (deg)	Ge/Ge Dist. in unloaded tool (Å)	Ge/Ge Load → unload relax (%)	Tool aspect ratio	Lowest Vibr. freq. (cm^{-1})
AdamGe22	2.97657	1.24200	1.94837	−0.0024	116.432	2.33589/S	−21.52	0.58614	140.13
AdamGe33	3.68211	1.23109	1.92538	0	129.532	2.38080/S	−35.34	0.40330	126.14
C100GeATD	3.10536	1.25187	1.96901	−12.6916	117.682	3.39435/T	+9.31	0.55945	187.47
C100GeATS	2.90700	1.24620	1.95320	0	115.160	2.59460/S	−10.75	0.60815	163.41
C100GeATSr5	3.30772	1.24718	1.98828	0	121.210	3.80842/T	+15.14	0.51411	158.55
C100GeATSr6	3.12800	1.24160	1.94675	0	118.980	2.44960/S	−21.69	0.54444	100.08
C100GeCTS	3.38180	1.23720	1.91771	0	123.997	2.52740/S	−25.26	0.47013	95.49
C110GeS	2.94671	1.24335	1.95571	0.0089	115.817	2.34034/S	−20.58	0.59745	154.59
C111Ge3	2.94420	1.24760	1.96726	0	115.544	3.15500/T	+7.16	0.60287	154.98
DCB55AGe	3.08857	1.25186	1.93927	0.0001	118.266	3.43249/T	+11.14	0.55302	181.41
DCB55BGe	2.98070	1.25861	1.97841	2.6694	120.319	3.43969/T	+15.40	0.59758	115.95
DCB55CGe	3.02914	1.25709	1.97082	0.0149	116.716	3.46946/T	+14.54	0.58116	130.85
DCB5Ge	3.07938	1.25068	1.92546	1.2858	118.347	2.84052/S	−7.76	0.55028	86.65
DCB57Ge	3.07120	1.24980	1.92090	0	118.301	2.81460/S	−8.36	0.55070	156.45
DCB65Ge	3.07960	1.24780	1.94086	0	118.158	2.68820/S	−12.71	0.55564	150.02
DCB6Ge	3.08240	1.24590	1.92322	0	118.520	2.56980/S	−16.63	0.54823	143.15
DCB75Ge	3.04539	1.24499	1.95349	0.0036	117.440	2.42784/S	−20.28	0.56929	95.37
DCBIceane7Ge	3.10750	1.24297	1.92205	0	119.015	2.38179/S	−23.35	0.54089	166.41
Diad3Ge22	3.00457	1.24506	1.96309	0.0001	116.625	2.58129/S	−14.09	0.58408	96.60
MCB5Ge	3.83060	1.23860	1.91667	0	132.545	4.05340/T	+5.82	0.36863	94.61
MCB55Ge	4.00585	1.24261	1.94773	0	135.182	4.92339/T	+22.91	0.34272	107.13
MCB57Ge	3.68760	1.23560	1.90595	0	130.035	2.49440/S	−32.36	0.39573	77.28
MCB75Ge	3.65640	1.23020	1.90322	0.1769	129.598	2.39440/S	−34.51	0.40108	39.75
TwistaneGe	3.13966	1.24290	1.93623	10.6353	119.062	2.39823/S	−23.62	0.53766	166.81

modest dimer wagging at 80–110 cm^{-1} for MCB5Ge, MCB55Ge, MCB57Ge and MCB75Ge and at 130–140 cm^{-1} for AdamGe22, AdamGe33, and Diad3Ge22. There is also a minor preference for tooltips exhibiting the smallest geometric relaxation between loaded and unloaded conditions (Table III, column 8) which may suggest greater dimensional stability during mechanosynthetic operations, although bonding to a rigid handle may reduce transitional geometric changes in all tools by stiffening the entire structure. Average unsigned change in Ge/Ge separation when moving from loaded to unloaded tooltip geometry is 17.92% for all 24 tooltips, ranging from an (unsigned) low of 5.82% for MCB5Ge to an (unsigned) high of 35.34% for AdamGe33.

Finally, a tooltip design that minimizes the risk of tool or workpiece poisoning by endogenous hydrogen migration is preferred. The first requirement is to provide the largest possible distance between the dimer C atoms and the nearest H atom in the tool base for the C$_2$-loaded tooltip (Fig. 5). All 24 tooltips have a minimum H/C$_2$ separation >2.70 Å (Table IV, column 2). While tooltips with a minimum H/C$_2$ separation less than ~2.60 Å (= 1.54 Å H$_3$Ge–H bond length +1.06 Å HCC–H bond length) might be regarded as particularly susceptible to H migration during nearby bond-breaking and bond-forming events, the passive barriers to H migration on clean diamond are nonetheless substantial, e.g., 3.31 eV (128 $k_B T$ at 300 K) crossing adjacent radical sites (2.50 Å) on the diamond

C(111) surface,[20] 2.05 eV (79 $k_B T$ at 300 K) cross-trough (3.09 Å) on the diamond C(110) surface,[21] and 2.06 eV (80 $k_B T$ at 300 K) cross-dimer (1.63 Å) on the diamond C(100) surface,[22] implying thermal migration times >10^{21} sec at 300 K. The second requirement is to ensure that the C$_2$ dimer (for the C$_2$-loaded tooltip; Table IV, column 3) or the Ge/Ge atoms (for the unloaded tooltip; Table IV, column 4) lie as high as possible above a plane perpendicular to the tool altitude containing the nearest H atoms in the tooltip base, thus offering the lowest probability of workpiece hydrogen poisoning when the tooltip is operated in proximity to a flat workpiece surface that presents
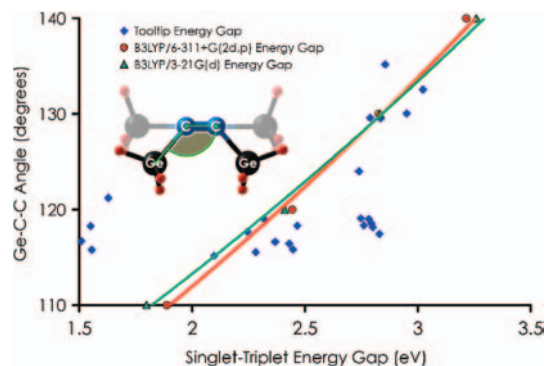
Fig. 4. Data points for Ge–C≡ bond angle as a function of singlet-triplet energy gap for tooltips in the horizontal configuration, overlaid by curves representing the same gap for a linear H$_3$Ge–C≡C–GeH$_3$ reference molecule (see insert) bent through a 110–140 deg range.
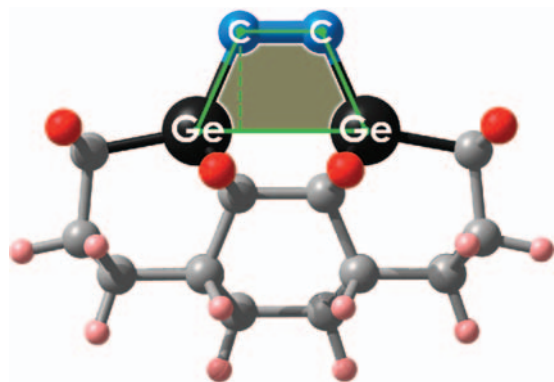
Fig. 5. Tooltip aspect ratio is defined as the height of the C_2 dimer line above the Ge/Ge line—approximated as the altitude (green dashed line) of the Ge–C–C–Ge trapezoid (green outline), assumed planar—expressed as a fraction of the Ge/Ge separation distance. The tooltip is susceptible to poisoning by the nearest hydrogen atoms (in red).

Fig. 6. Selection of Ge-substituted dimer placement tooltip motifs with best overall characteristics: (A) C100GeATSr5, (B) C100GeATS, (C) DCB55AGe, and (D) DCB6Ge.

dangling bonds. Designs featuring an H atom bonded to a Ge atom (as in AdamGe22, AdamGe33, C110GeS, DCBIceane7Ge, Diad3Ge22, TwistaneGe) might experience decreased tooltip recharging reliability due to steric migration of the H, though in a full tool + handle design the H–Ge segments may be replaced with stiffer C–Ge bonded handle structures.

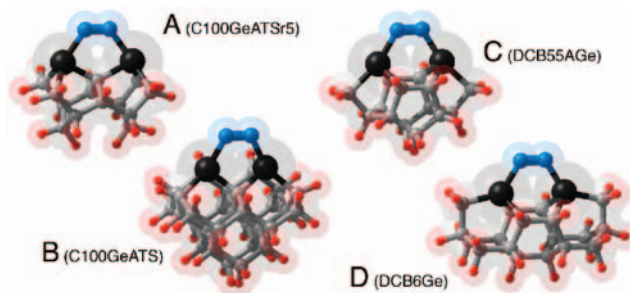Comparing DCB and MCB motifs, MCB5X and DCB5X/DCB6X tend to favor the desired horizontal dimer, whereas MCB6X/MCB7X and DCB7X tend to favor carbenization. While Ge atoms are 0.6–1.0 Å farther apart in the horizontal MCB motifs than in the horizontal DCB motifs, the decrease in the Ge/Ge separation from horizontal to carbene singlet is −0.3 Å to −0.5 Å greater for the MCB motifs. This larger change in Ge/Ge separation indicates that the MCB frames are less rigid than the DCB frames, providing enough flex to orient Ge atoms to better match the preferred binding geometry of the carbene. Adding atoms to the base ring has no apparent effect on the propensity to carbenize. DCB and MCB motifs differ little in dimer transfer exoergicity but DCB offers a 50% higher aspect ratio, 50% greater dimer height above H atoms in the base, and 70% higher minimum vibrational frequency.

The prioritization of design objectives will determine which tooltip is best in a given circumstance.

Table IV. Ge-based dimer placement tooltip motifs ranked for hydrogen poisoning risk (lowest-risk motifs at top of table; rank order based on 3-column sum). Values are for horizontal or discharged singlet structures.

Tooltip	Minimum distance from dimer C atom to nearest H atom in loaded tooltip base (Å)	Height of C_2 dimer above highest H atom in loaded tooltip base (Å)	Height of Ge/Ge atoms above highest H atom in unloaded tooltip base (Å)
C100GeATSr5	3.53946	2.39805	0.77696
C100GeATS	3.54574	2.13045	0.76177
DCB5Ge	3.31647	2.15583	0.52469
DCB55AGe	3.35613	2.17411	0.45480
DCB57Ge	3.35331	2.05651	0.31037
MCB55Ge	3.61630	1.60622	0.40142
C100GeATSr6	3.54992	1.88123	−0.05689
DCB65Ge	3.15472	1.89795	0.14616
MCB5Ge	3.48971	1.45841	0.13396
DCB6Ge	3.41239	1.58290	−0.31166
Diad3Ge22	2.77335	1.64217	0.18404
DCB55CGe	3.06649	1.68069	−0.10151
AVERAGE	**3.16859**	**1.59362**	**−0.25545**
C111Ge3	2.90805	1.69851	−0.05317
MCB57Ge	3.36251	1.40971	−0.47700
DCB55BGe	2.90711	1.42475	−0.43467
TwistaneGe	2.90560	1.59883	−0.78189
DCBIceane7Ge	2.92895	1.55801	−0.82796
AdamGe22	2.93694	1.58248	−0.93830
C100GeATD	2.73808	1.30976	−0.50943
C100GeCTS	3.43687	0.98688	−0.93241
C110GeS	2.76926	1.53038	−0.91049
DCB75Ge	2.90347	1.06741	−1.04072
AdamGe33	2.91764	1.06188	−1.13452
MCB75Ge	3.15762	0.35364	−1.31440

C100GeATSr5 (Fig. 6(A)) provides the highest transfer energy and the best protection against hydrogen poisoning of any tooltip motif presented here, along with a relatively high vibrational frequency and a good aspect ratio. C100GeATS (Fig. 6(B)) provides the highest aspect ratio among all tooltips studied here, along with the second-best protection against hydrogen poisoning, a high vibrational frequency and a good transfer energy. DCB55AGe (Fig. 6(C)) provides the highest vibrational frequency among these tooltips, along with a high aspect ratio, a very good transfer energy, and good hydrogen poisoning protection. DCB6Ge (Fig. 6(D)) combines high aspect ratio and high vibrational frequency with adequate transfer energy and above-average hydrogen poisoning protection. Of the four motifs mentioned above, C100GeATS and DCB6Ge are most conveniently mated to a larger diamond lattice handle structure, and DCB6Ge is already the most-studied C₂ dimer placement tool reported in the DMS literature.

Regarding the utility of a specific horizontal dimer placement tool on a specific diamond surface, to date only the stable DCB6Ge tooltip motif[6] has been validated to achieve successful room-temperature deposition of C₂ dimers on any of the three principal diamond lattice planes, in this case via an extensive stepwise *ab initio* (DFT/GGA) molecular dynamics analysis[7–9] using nonlocal plane-wave basis functions with a 200-atom model of the clean C(110) diamond surface. Such detailed studies of tooltip dynamic stability and dimer deposition efficacy on all diamond lattice planes for the other tooltips reported here, as well as for alternative dimer placement tooltip motifs that have been proposed elsewhere,[24] have not yet begun and should be undertaken as soon as possible.

References

1. D. M. Eigler and E. K. Schweizer, *Nature* 344, 524 (**1990**).
2. N. Oyabu, O. Custance, I. Yi, Y. Sugawara, and S. Morita, *Phys. Rev. Lett.* 90, 176102 (**2003**).
3. S. P. Walch and R. C. Merkle, *Nanotechnology* 9, 285 (**1998**).
4. K. E. Drexler, Nanosystems: Molecular Machinery, Manufacturing, and Computation, John Wiley and Sons, New York (**1992**).
5. F. N. Dzegilenko, D. Srivastava, and S. Saini, *Nanotechnology* 9, 325 (**1998**).
6. R. C. Merkle and R. A. Freitas, Jr., *J. Nanosci. Nanotechnol.* 3, 319 (**2003**).
7. J. Peng, R. A. Freitas, Jr., and R. C. Merkle, *J. Comput. Theor. Nanosci.* 1, 62 (**2004**).
8. D. J. Mann, J. Peng, R. A. Freitas, Jr., and R. C. Merkle, *J. Comput. Theor. Nanosci.* 1, 71 (**2004**).
9. J. Peng, R. A. Freitas, Jr., R. C. Merkle, J. R. Von Ehr, J. N. Randall, and G. D. Skidmore, *J. Comput. Theor. Nanosci.* 3, 28 (**2006**).
10. H. Schäfer, W. Saak, and M. Weidenbruch, *Angew. Chem. Int. Ed.* 39, 3702 (**2000**).
11. C. Glidewell and D. C. Liles, *Acta Cryst.* B38, 1320 (**1982**).
12. M. Weidenbruch, *Angew. Chem. Int. Ed.* 42, 2222 (**2003**).
13. John Drake, Organogermanium Compounds, Springer-Verlag, New York (**1994**).
14. G. Z. Rappoport (ed.), The Chemistry of Organic Germanium, Tin and Lead Compounds, John Wiley and Sons, New York (**2003**), Vol. 2.
15. N. Auner and J. Weis (eds.), Organosilicon Chemistry: From Molecules to Materials, VCH and John Wiley and Sons, New York, Vols. I (**1994**), II (**1995**), III (**1998**), IV (**2000**), V (**2003**).
16. E. W. Krahe, R. Mattes, K.-F. Tebbe, H. G. v. Schnering, and G. Fritz, *Z. Anorg. Allg. Chem.* 393, 74 (**1972**).
17. R. A. Freitas, Jr., A simple tool for positional diamond mechanosynthesis, and its method of manufacture, U.S. Provisional Patent Application No. 60/543,802; U.S. Patent Pending (**2005**).
18. M. J. Frisch, G. W. Trucks, H. B. Schlegel, G. E. Scuseria, M. A. Robb, J. R. Cheeseman, V. G. Zakrzewski, J. A. Montgomery, Jr., R. E. Stratmann, J. C. Burant, S. Dapprich, J. M. Millam, A. D. Daniels, K. N. Kudin, M. C. Strain, O. Farkas, J. Tomasi, V. Barone, M. Cossi, R. Cammi, B. Mennucci, C. Pomelli, C. Adamo, S. Clifford, J. Ochterski, G. A. Petersson, P. Y. Ayala, Q. Cui, K. Morokuma, P. Salvador, J. J. Dannenberg, D. K. Malick, A. D. Rabuck, K. Raghavachari, J. B. Foresman, J. Cioslowski, J. V. Ortiz, A. G. Baboul, B. B. Stefanov, G. Liu, A. Liashenko, P. Piskorz, I. Komaromi, R. Gomperts, R. L. Martin, D. J. Fox, T. Keith, M. A. Al-Laham, C. Y. Peng, A. Nanayakkara, M. Challacombe, P. M. W. Gill, B. Johnson, W. Chen, M. W. Wong, J. L. Andres, C. Gonzalez, M. Head-Gordon, E. S. Replogle, and J. A. Pople, *Gaussian 98*, Revision A.11, Gaussian Inc., Pittsburgh, PA (**2001**).
19. J. B. Foresman and A. Frisch, *Exploring Chemistry with Electronic Structure Methods: A Guide to Using Gaussian*, 2nd edn., Gaussian Inc., Pittsburgh, PA (**1996**).
20. X. Y. Chang, D. L. Thompson, and L. M. Raff, *J. Chem. Phys.* 100, 1765 (**1994**).
21. M. I. Heggie, C. D. Latham, B. Jones, and P. R. Briddon, *Proceedings of the Fourth International Symposium on Diamond Materials*, edited by K. V. Ravi and J. P. Dismukes, The Electrochemical Society, Pennington, NJ (**1995**), pp. 643–648.
22. E. J. Dawnkaski, D. Srivastava, and B. J. Garrison, *J. Chem. Phys.* 102, 9401 (**1995**).
23. Geoff Leach, *Nanotechnology* 7, 197 (**1996**).
24. D. G. Allis and K. E. Drexler, *J. Comput. Theor. Nanosci.* 2, 45 (**2005**).
25. A. D. Becke, *J. Chem. Phys.* 98, 5648 (**1993**).
26. J. S. Binkley, J. A. Pople, and W. J. Hehre, *J. Am. Chem. Soc.* 102, 939 (**1980**).
27. R. Krishnan, J. S. Binkley, R. Seeger, and J. A. Pople, *J. Chem. Phys.* 72, 650 (**1980**).
28. M. J. S. Dewar, E. G. Zoebisch, E. F. Healy, and J. J. P. Stewart, *J. Am. Chem. Soc.* 107, 3902 (**1985**).

10

*J. Comput. Theor. Nanosci. 4, 1–10, **2007***